ECS Journal of Solid State
Science and Technology

OPEN ACCESS

Static Dielectric Constant of β-Ga_2O_3 Perpendicular to the Principal Planes (100), (010), and (001)

To cite this article: A. Fiedler *et al* 2019 *ECS J. Solid State Sci. Technol.* **8** Q3083

JSS Focus Issue on Gallium Oxide Based Materials and Devices

Static Dielectric Constant of β-Ga_2O_3 Perpendicular to the Principal Planes (100), (010), and (001)

A. Fiedler, [z] **R. Schewski, Z. Galazka, and K. Irmscher**[z]

Leibniz-Institut für Kristallzüchtung, 12489 Berlin, Germany

The relative static dielectric constant ε_r of β-Ga_2O_3 perpendicular to the planes (100), (010), and (001) is determined in the temperature range from 25 K to 500 K by measuring the AC capacitance of correspondingly oriented plate capacitor structures using test frequencies of up to 1 MHz. This allows a direct quantification of the static dielectric constant and a unique direction assignment of the obtained values. At room temperature, ε_r perpendicular to the planes (100), (010), and (001) amounts to 10.2 ± 0.2, 10.87 ± 0.08, and 12.4 ± 0.4, respectively, which clearly evidence the anisotropy expected for β-Ga_2O_3 due to its monoclinic crystal structure. An increase of ε_r by about 0.5 with increasing temperature from 25 K to 450 K was found for all orientations. Our ε_r data resolve the inconsistencies in the previously available literature data with regard to absolute values and their directional assignment and therefore provide a reliable basis for the simulation and design of devices.

 [DOI: 10.1149/2.0201907jss]

Manuscript received February 15, 2019. Published March 2, 2019. *This paper is part of the JSS Focus Issue on Gallium Oxide Based Materials and Devices.*

Monoclinic gallium sesquioxide (β-Ga_2O_3) has gained overwhelming interest in recent years due to its promising properties for high power electronics.[1] Due to the large bandgap of about 4.8 eV,[2] a breakdown electric field as high as 8 MV/cm can be estimated. Combined with the feasibility of n-type doping in the range from 10^{13} cm^{-3} to 10^{20} cm^{-3}, and a reasonable electron mobility of up to 200 cm^2/Vs,[3,4,5] β-Ga_2O_3 might outperform GaN and SiC as a material for low-frequency unipolar vertical power switches.[6] To evaluate the potential of β-Ga_2O_3 for power electronics, several demonstrator devices such as field effect transistors[7–12] and Schottky barrier diodes were fabricated.[13,14] Such devices are realized on the technologically most relevant surfaces of β-Ga_2O_3, i.e. (100), (010), or (001). Hence, the direction of the electric field in the space charge region underneath the Schottky contacts or the gates is primarily perpendicular to one of these planes. For device design, in particular for the calculation of the electric potential and the field distribution in the active region, the relative static dielectric constant ε_r has to be known. Due to the monoclinic structure of β-Ga_2O_3, ε_r is expected to be anisotropic. Up to now however, device related experiments and simulations have assumed an average static dielectric constant $\langle\varepsilon_r\rangle \approx 10$ disregarding the anisotropy. This average value traces back to reports by Hoeneisen et al., who measured for single crystals $\varepsilon_r = 10.2 \pm 0.3$ perpendicular to (100),[15] or by Passlack et al. who measured $\langle\varepsilon_r\rangle$ between 9.93 ± 0.39 and 10.2 ± 0.6 for amorphous films[16] as well as $\langle\varepsilon_r\rangle = 9.57$ for polycrystalline films.[17] Recently, however, an experimental study by ellipsometry[18] and calculations by density functional theory[19–21] have revealed that there is a significant anisotropy in the relative static dielectric constant. Although these reports roughly agree in the magnitude of the principal components of the static dielectric tensor, they are inconsistent with respect to the crystal axis assignment of the components. Hence, providing reliable data of the static dielectric constant's magnitude and direction dependence is still an issue for a correct design and simulation of β-Ga_2O_3 devices.

Here, we report on AC capacitance measurements of the relative static dielectric constant ε_r of β-Ga_2O_3 perpendicular to the (100), (010), and (001) plane in the temperature range from 25 K to 500 K by using correspondingly oriented plate capacitor structures. Such measurements allow a direct determination of ε_r from the sample capacitance and geometry. The values obtained should be better suited for purposes of device simulation than those available so far. Our results indeed confirm an anisotropy of ε_r of up to 25% between the different crystal orientations, but more important, resolve the ambiguity in the orientation assignment.

Experimental

The β-Ga_2O_3 crystals used in the present study were either grown by the Czochralski (Cz) method at the Leibniz-Institut für Kristallzüchtung or by the edge-defined, film-fed growth method (EFG) at Tamura Corp., Japan. To obtain semi-insulating material, the unintentional n-type doping of β-Ga_2O_3 is compensated by magnesium (Cz) or iron (EFG) doping. A detailed description for the EFG[22] and the Cz[23–25] growth can be found elsewhere. The Cz crystals were oriented by Laue diffraction and subsequently sawed, cleaved, and polished to obtain samples with the surface orientations (100) and (001), corresponding to the surface normals **a*** and **c***, respectively. For the (010) oriented sample (surface normal **b**) a substrate wafer from an EFG crystal was used. Figure 1a illustrates the axis assignment with respect to the unit cell of β-Ga_2O_3. Figure 1b shows a scheme of the plate capacitor structure used for the AC capacitance measurements. Contacts were deposited by electron beam evaporation of Ti (20 nm) and Au (50 nm) in vacuum at a pressure of few 10^{-6} mbar using circular shadow masks aligned congruently on opposite sites. The area A of the contacts and its uncertainty were determined by polygonal area analysis of microphotographs. The thickness d of the samples was

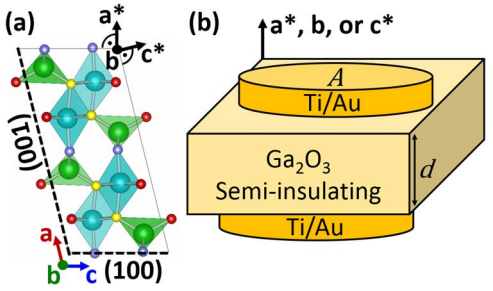

Figure 1. (a) The monoclinic unit cell of β-Ga_2O_3 is illustrated using VESTA.[28] The (100) and the (001) planes are indicated by dashed lines on which **a*** and **c*** are perpendicular, respectively. The (010) plane is perpendicular to the viewing direction **b**. (b) Scheme of the plate capacitor structure used in the AC capacitance measurements. A is the area of the contact and d is the thickness of the sample. The contacts on the semi-insulating β-Ga_2O_3 are either fabricated on the planes (100), (010), or (001).

[z]E-mail: Andreas.fiedler@ikz-berlin.de; Klaus.irmscher@ikz-berlin.de

Table I. The experimentally determined values for the area A of the contact, the thickness d of the sample and the capacitance C of the plate capacitor structure at room temperature on the three different planes (100), (010), and (001) are shown.

Surface orientation of the sample	(100)	(010)	(001)
A [mm^2]	53.0 ± 0.2	53.2 ± 0.2	23.0 ± 0.2
d [μm]	325 ± 5	509 ± 5	110 ± 3
C [pF]	14.71 ± 0.04	10.06 ± 0.03	22.92 ± 0.06

measured using a commercial digital dial indicator (Mitutoyo Corp ID-S112SB) with a resolution of 1 μm and an accuracy of 3 μm. The error of d was calculated by the root mean square of the indicator's accuracy and the statistical error from a number of measurements at different spots on the sample. The capacitance was measured using a HP4284A precision LCR meter (Hewlett Packard). We made sure that the loss tangent tan(δ) was smaller than 0.1 to neglect the influence of the conductance on the AC capacitance measurement. The capacitance C was independent from the frequency in the range from 20 kHz to 1 MHz and also independent from the DC bias between −100 V and +100 V. Thus all prerequisites were fulfilled to use the AC capacitance measuring method. For the determination of the relative static dielectric constant ε_r, we measured the capacitance at zero bias, to reduce the leakage current at elevated temperatures. A test frequency of 1 MHz was chosen since the LCR meter has the highest accuracy in this range and the loss tangent tan(δ) is smaller with larger frequencies, which mainly plays a role for higher temperatures.

The temperature dependence of the capacitance was measured between 25 K and 500 K in a Janis CCS-400H/204N closed cycle refrigerator cryostat. The capacitance of the setup (without sample) was determined to be 0.85 pF and was taken into account for the zero correction.

Results and Discussion

The experimentally determined values for the contact area, the sample thickness and the capacitance at room temperature on the three different planes (100), (010), and (001) are summarized in Table I. The relative static dielectric constant ε_r is calculated via the formula for plate capacitors

$$\varepsilon_r = \frac{C \cdot d}{A \cdot \varepsilon_0}, \qquad [1]$$

where $\varepsilon_0 = 8.854 \times 10^{-12}$ F/m is the vacuum permittivity.

The resulting ε_r perpendicular to the (100), (010), and (001) plane between 25 K and 500 K is plotted in Figure 2. One-sigma error bars are indicated for each measurement by the shaded areas. The relative error in the sample thickness is dominating the calculated error of ε_r. A significant difference of ε_r up to 25% between the three different orientations is found. However, only a weak temperature dependence is observed for all orientations with ε_r increasing by about 0.5 from 25 K to 450 K (Table II). A reliable measurement of the capacitance above 500 K was not possible due to the increased leakage current leading to a loss tangent tan(δ) > 0.1.

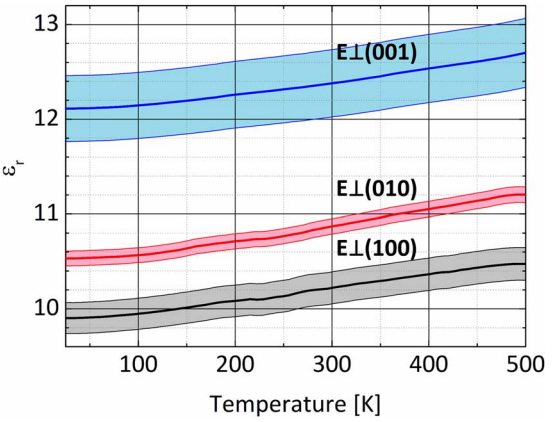

Figure 2. The relative static dielectric constant versus the temperature perpendicular to (100), (010) and (001) between 25 K and 500 K. Selected values are presented in Table II.

The resulting ε_r perpendicular to the (100), (010), and (001) plane at room temperature is summarized and compared to literature data in Table III. For ε_r perpendicular to the (100) plane, we confirm the experimental result by Hoeneisen et al.[15] They determined ε_r also using AC capacitance measurements, but for crystals grown by the Verneuil technique as well as for flux grown crystals suggesting that extrinsic effects are of minor importance. ε_r perpendicular to the (010) and (001) planes were up to now only determined by ellipsometry[18] and density functional theory calculations[19–21]. They used a Cartesian system (**a**, **b**, **c***) for the ε_r tensor, so that ε_r perpendicular to (100) measured by us deviates from their value with **E** ∥ **a**, which, in our opinion, does not make too much difference and cannot be the reason for the deviations discussed in the following. As the comparison in Table III shows, these reports and our results fairly agree in the magnitude of ε_r. However, the order of the ε_r values with respect to the crystal axes does not agree. Considering the deviations in the ε_r values based on DFT calculations, it does not make sense to compare the absolute values with ours. The ellipsometry results of Schubert et al.[18] disagree with ours within the error bars. They used a generalized Lyddane-Sachs-Teller relation (LST) to determine the relative static dielectric constant in the monoclinic system. The LST is an indirect approach to determine ε_r from the phonon modes of an ionic crystal, which may fail in the presence of free charge carriers. In their study β-Ga_2O_3:Sn single crystals with net donor concentrations of (2 – 9) × 10^{18} cm^{-3} were used.[18] Since Sn is a shallow donor in β-Ga_2O_3[26] nearly full ionization at room temperature can be assumed. Hence, free charge carriers are present in the samples they used, which could

Table II. The relative static dielectric constant ε_r perpendicular to the planes (100), (010), and (001) of the monoclinic lattice of β-Ga_2O_3 at different temperatures.

	ε_r for **E** perpendicular to		
	(100)	(010)	(001)
T = 25 K	9.9 ± 0.2	10.53 ± 0.08	12.1 ± 0.4
T = 150 K	10.0 ± 0.2	10.64 ± 0.08	12.2 ± 0.4
T = 300 K	10.2 ± 0.2	10.87 ± 0.08	12.4 ± 0.4
T = 450 K	10.4 ± 0.2	11.14 ± 0.08	12.6 ± 0.4

Table III. The relative static dielectric constant ε_r perpendicular to the (100), (010) and (001) plane of the monoclinic lattice of β-Ga_2O_3 at room temperature.

	ε_r for **E** perpendicular to		
	(100)	(010)	(001)
This work	10.2 ± 0.2	10.87 ± 0.08	12.4 ± 0.4
Exp. Ref. 15	10.2 ± 0.3	-	-
Exp. Ref. 18	12.(7)[a]	11.(2)	10.(9)
Theory Ref. 19	10.84[b]	11.49[b]	13.89[b]
Theory Ref. 20	11.4[a]	11.0	15.0
Theory Ref. 21	11.88[a]	9.22	12.61

[a]**E** ∥ **a** ∦ **a***
[b]crystal axes assignment unknown

explain the discrepancies with our results. There are also reports on polycrystalline and amorphous films, that give an average value over all orientations of $\langle\varepsilon_r\rangle = 9.57$,[17] $\langle\varepsilon_r\rangle = 9.93 \pm 0.39$, and $\langle\varepsilon_r\rangle = 10.2 \pm 0.6$.[16] The average of the relative static dielectric constant over all orientations is in our case $\langle\varepsilon_r\rangle = 11.2 \pm 0.2$. The larger value can be explained by the fact that amorphous networks are less densely packed than the crystalline phase resulting in a significantly lower relative static dielectric constant for the amorphous phase. This was shown especially for binary and mixed oxides.[27]

Summary

The relative static dielectric constant ε_r of β-Ga_2O_3 perpendicular to the planes (100), (010), and (001) has been determined at room temperature to 10.2 ± 0.2, 10.87 ± 0.08, and 12.4 ± 0.4, respectively. ε_r increased by about 0.5 with increasing temperature from 25 K to 450 K for all orientations. ε_r was directly determined from AC capacitance measurements and the geometry of correspondingly oriented plate capacitor structures. This makes the orientation assignment clearly comprehensible. Since demonstrator devices were realized on β-Ga_2O_3 surfaces with one of the three principal orientations (100), (010), or (001), the electric field direction in the space charge region underneath the Schottky contacts or the gates is essentially perpendicular to one of these planes. Therefore, the values reported here allow an exact device design.

Acknowledgment

The Authors express their gratitude to A. Kwasniewski, U. Juda and K. Banse for the technical support. The authors also thank M. Albrecht, H. von Wenckstern and L. Vines for the discussion. One of the authors (R. Schewski) acknowledges funding by German Research Foundation (DFG) (grant No. GA 2057/2-1). This work was performed in the framework of GraFOx, a Leibniz-ScienceCampus partially funded by the Leibniz association.

ORCID

A. Fiedler https://orcid.org/0000-0003-3404-0804

References

1. S. J. Pearton, F. Ren, M. Tadjer, and J. Kim, *J. Appl. Phys.*, **124**, 220901 (2018).
2. C. Janowitz, V. Scherer, M. Mohamed, A. Krapf, H. Dwelk, R. Manzke, Z. Galazka, R. Uecker, K. Irmscher, R. Fornari, M. Michling, D. Schmeißer, J. R. Weber, J. B. Varley, and C. G. Van De Walle, *New J. Phys.*, **13**, (2011).
3. H. Murakami, K. Nomura, K. Goto, K. Sasaki, K. Kawara, Q. Tu Thieu, R. Togashi, Y. Kumagai, M. Higashiwaki, A. Kuramata, S. Yamakoshi, B. Monemar, and A. Koukitu, *Appl. Phys. Express*, **8**, 015503 (2015).
4. K. D. Leedy, K. D. Chabak, V. Vasilyev, D. C. Look, J. J. Boeckl, J. L. Brown, S. E. Tetlak, A. J. Green, N. A. Moser, A. Crespo, D. B. Thomson, R. C. Fitch, J. P. McCandless, and G. H. Jessen, *Appl. Phys. Lett.*, **111**, 012103 (2017).
5. N. Ma, N. Tanen, A. Verma, Z. Guo, T. Luo, H. (Grace) Xing, and D. Jena, *Appl. Phys. Lett.*, **109**, 212101 (2016).
6. J. Y. Tsao, S. Chowdhury, M. A. Hollis, D. Jena, N. M. Johnson, K. A. Jones, R. J. Kaplar, S. Rajan, C. G. Van de Walle, E. Bellotti, C. L. Chua, R. Collazo, M. E. Coltrin, J. A. Cooper, K. R. Evans, S. Graham, T. A. Grotjohn, E. R. Heller, M. Higashiwaki, M. S. Islam, P. W. Juodawlkis, M. A. Khan, A. D. Koehler, J. H. Leach, U. K. Mishra, R. J. Nemanich, R. C. N. Pilawa-Podgurski, J. B. Shealy, Z. Sitar, M. J. Tadjer, A. F. Witulski, M. Wraback, and J. A. Simmons, *Adv. Electron. Mater.*, **4**, 1 (2018).
7. M. Higashiwaki, K. Sasaki, A. Kuramata, T. Masui, and S. Yamakoshi, *Appl. Phys. Lett.*, **100**, 013504 (2012).
8. M. Higashiwaki, K. Sasaki, A. Kuramata, T. Masui, and S. Yamakoshi, *Phys. Status Solidi A*, **211**, 21 (2014).
9. A. J. Green, K. D. Chabak, E. R. Heller, R. C. Fitch, M. Baldini, A. Fiedler, K. Irmscher, G. Wagner, Z. Galazka, S. E. Tetlak, A. Crespo, K. Leedy, and G. H. Jessen, *IEEE Electron Device Lett.*, **37**, 902 (2016).
10. M. Higashiwaki, K. Sasaki, H. Murakami, Y. Kumagai, A. Koukitu, A. Kuramata, T. Masui, and S. Yamakoshi, *Semicond. Sci. Technol.*, **31**, 034001 (2016).
11. W. S. Hwang, A. Verma, H. Peelaers, V. Protasenko, S. Rouvimov, H. G. Xing, A. Seabaugh, W. Haensch, C. G. Van de Walle, Z. Galazka, M. Albrecht, R. Fornari, and D. Jena, *Appl. Phys. Lett.*, **104**, 203111 (2014).
12. Z. Hu, K. Nomoto, W. Li, N. Tanen, K. Sasaki, A. Kuramata, T. Nakamura, D. Jena, and H. G. Xing, *IEEE Electron Device Lett.*, **39**, 869 (2018).
13. K. Sasaki, M. Higashiwaki, A. Kuramata, T. Masui, and S. Yamakoshi, *IEEE Electron Device Lett.*, **34**, 493 (2013).
14. K. Konishi, K. Goto, H. Murakami, Y. Kumagai, A. Kuramata, S. Yamakoshi, and M. Higashiwaki, *Appl. Phys. Lett.*, **110**, 103506 (2017).
15. B. Hoeneisen, C. A. Mead, and M.-A. Nicolet, *Solid State Electron.*, **14**, 1057 (1971).
16. M. Passlack, N. E. J. Hunt, E. F. Schubert, G. J. Zydzik, M. Hong, J. P. Mannaerts, R. L. Opila, and R. J. Fischer, *Appl. Phys. Express*, **64**, 2715 (1994).
17. G. Schmitz, P. Gassmann, and R. Franchy, *J. Appl. Phys.*, **83**, 2533 (1998).
18. M. Schubert, R. Korlacki, S. Knight, T. Hofmann, S. Schöche, V. Darakchieva, E. Janzén, B. Monemar, D. Gogova, Q.-T. Thieu, R. Togashi, H. Murakami, Y. Kumagai, K. Goto, A. Kuramata, S. Yamakoshi, and M. Higashiwaki, *Phys. Rev. B*, **93**, 125209 (2016).
19. B. Liu, M. Gu, and X. Liu, *Appl. Phys. Lett.*, **91**, 172102 (2007).
20. K. Ghosh and U. Singisetti, *Appl. Phys. Lett.*, **109**, 072102 (2016).
21. Y. Kang, K. Krishnaswamy, H. Peelaers, and C. G. Van De Walle, *J. Physics. Condens. Matter*, **29**, 234001 (2017).
22. H. Aida, K. Nishiguchi, H. Takeda, N. Aota, K. Sunakawa, and Y. Yaguchi, *Jpn. J. Appl. Phys.*, **47**, 8506 (2008).
23. Z. Galazka, R. Uecker, K. Irmscher, M. Albrecht, D. Klimm, M. Pietsch, M. Brützam, R. Bertram, S. Ganschow, and R. Fornari, *Cryst. Res. Technol.*, **45**, 1229 (2010).
24. Z. Galazka, K. Irmscher, R. Uecker, R. Bertram, M. Pietsch, A. Kwasniewski, M. Naumann, T. Schulz, R. Schewski, D. Klimm, and M. Bickermann, *J. Cryst. Growth*, **404**, 184 (2014).
25. Z. Galazka, R. Uecker, D. Klimm, K. Irmscher, M. Naumann, M. Pietsch, A. Kwasniewski, R. Bertram, S. Ganschow, and M. Bickermann, *ECS J. Solid State Sci. Technol.*, **6**, Q3007 (2017).
26. J. B. Varley, J. R. Weber, A. Janotti, and C. G. Van de Walle, *Appl. Phys. Lett.*, **97**, 142106 (2010).
27. E. Gusev, *Defects in High-k Gate Dielectric Stacks: Nano-Electronic Semiconductor Devices*, (Springer Netherlands, 2006).
28. K. Momma and F. Izumi, *J. Appl. Crystallogr.*, **41**, 653 (2008).